

Lin Tian<sup>1</sup>, Gerry Heymsfield<sup>2</sup>, Lihua Li<sup>1</sup>, and Xiaowen Li<sup>1</sup>

<sup>1</sup>Goddard Earth Science and Technology Center, University of Maryland, Baltimore

<sup>2</sup>NASA Goddard Space Flight Center

## 1. Introduction

The melting band has been a distinctive feature of the radar measurements of precipitation. It is primarily caused by the rapid increases in the dielectric constant of hydrometeors at the top of the melting layer followed by an increase of the fall velocity of melting snowflakes toward the bottom of the melting layer. The melting band in stratiform rain, originally studied at cm wavelength, is characterized by an enhancement of the radar reflectivity. However, later observations made at mm wavelength (Lhermitte 1988) often show the absence of the bright band and, in some cases, a decrease of the reflectivity in the melting layer, namely, a dark band. Such phenomena were attributed to the dominance of non-Rayleigh scattering effects at mm wavelength (Sassen et al. 2005).

During the Cirrus Regional Study of Tropical and Cirrus Layers (CRYSTAL) Florida Area Cirrus Experiment field campaign in southern Florida, light stratiform rain with rainfall rate less than 2 mm/hr were observed by 3.2 mm and 3.2 cm wavelength airborne Doppler radars. A method that uses both reflectivity and Doppler velocity to retrieve the rain rate below the melting layer has shown promising results (Tian et al. 2005). In this paper, we focus on regions in and above the melting layer. We are attempting to understand the observations in terms of particle melting processes and scattering cross-sections of melting particles at the two wavelengths. Such understanding is important for improving the rainfall retrieval with dual-wavelength Doppler radars.

## 2. Observations

Fig. 1 shows a flight line from July 2002. Fig. 2 is a profile from Fig. 1. The reflectivity profile at 3.2 cm wavelength is typical for the stratiform rain.

That is, it increases as height decreases, an indication of growing ice particles by aggregation. It then increases as particles start melting, reaching a maximum in the melting band, and then decreases and is stabilized in rain. The corresponding profile at 3.2 mm wavelength decreases as height decreases, an indication that ice particles are no longer the Rayleigh scatters. A minimum is reached at top of the melting band, indicating the onset of the melting. The reflectivity then increases to a maximum in the melting layer at the same height as that of maximum reflectivity at the cm-wavelength and decreases downward. The further decrease in rain is due to the large attenuation at mm-wavelength.

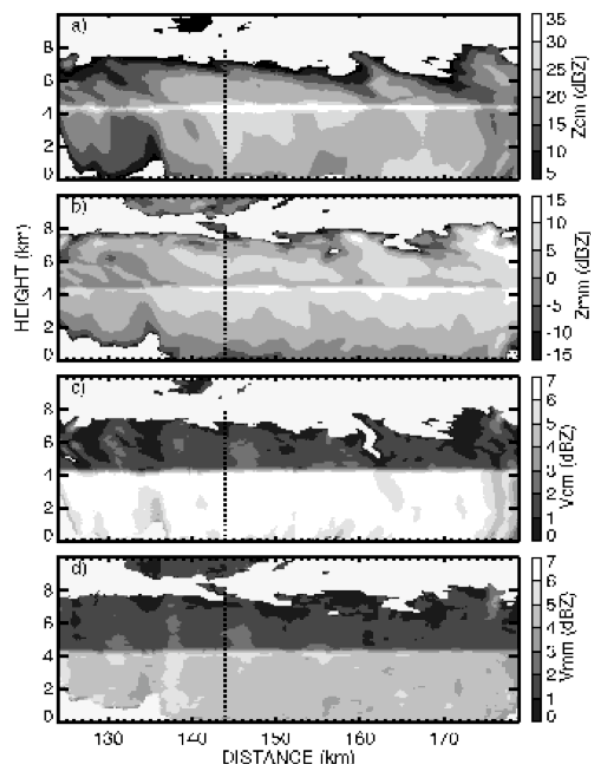


Fig. 1 Observed a) reflectivity from EDOP ( $Z_{cm}$ ) and b) CRS ( $Z_{mm}$ ); Doppler velocity from c) EDOP ( $V_{cm}$ ) and d) CRS ( $V_{mm}$ ).

Corresponding author's address: Lin Tian, GSFC/NASA, Mail Code 912, Greenbelt, MD 20771; e-mail: [tian@agnes.gsfc.nasa.gov](mailto:tian@agnes.gsfc.nasa.gov)

The Doppler velocities in the snow are more or less the same at both wavelengths. As melting starts, the velocities start increasing with distance downwards and stabilize in the rain region with greater velocities at the cm wavelength. The stabilization occurs earlier for the mm-wavelength. Complete melting is probably achieved where the cm wavelength velocity has stabilized to the rain value. This difference has been interpreted as the different reflectivity weighting toward the different sizes for the mm and cm wavelengths.

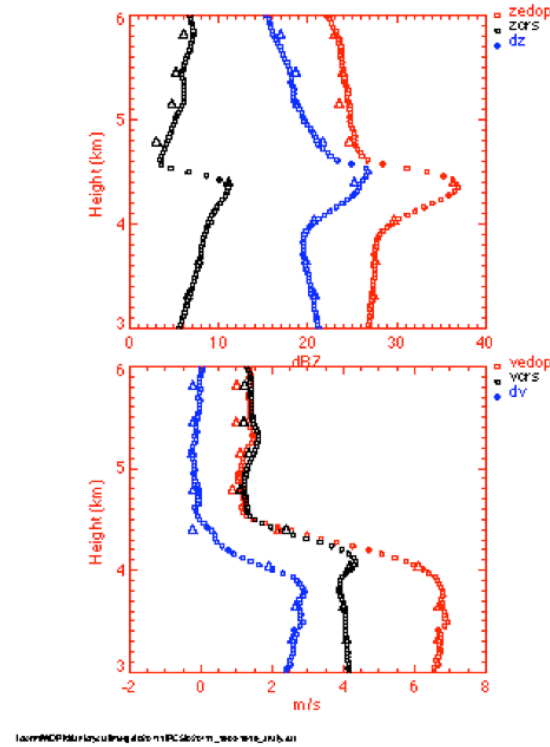


Fig. 2 a) Profile of Reflectivity at 10 (red) and 94 GHz (black) and the difference ( $dz = zedop - zcrs$ ). b) Doppler velocity at 10 and 94 GHz and the difference ( $dv = vedop - vcrs$ ).

### 3. Results from theoretical calculation

The back-scattering cross-section of the melting particles depends not only on the size and refractive index but also on the density of the particles. In addition, both the particle size distribution and terminal velocity are changing during the melting process. We start with a simple one-dimensional melting model with the following assumptions: a) Steady state rainfall, no breakup or aggregation, b) density of the snow flake decreasing with increase size, and c) exponential drop size distribution in rain, and d) spherical melting snow flakes are covered with water. Figure 3 shows fall velocity of the melting the

melting particles and fraction of melting water as a function of height. The actual melting starts at about 4.4 km height. It shows that small particles melt faster than the bigger particles as expected.

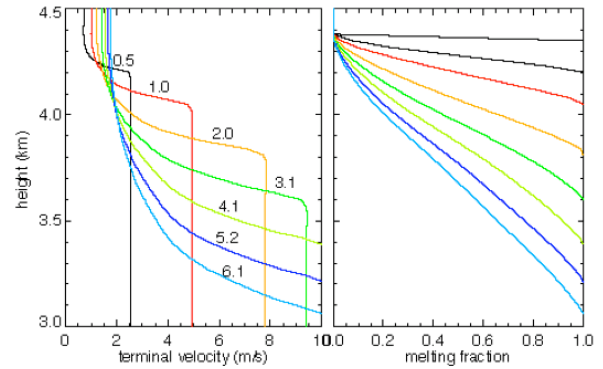


Fig. 3 Left: Profile of the fall velocity of the melting particles; Right: Profile of melting ratio for selected melted diameters

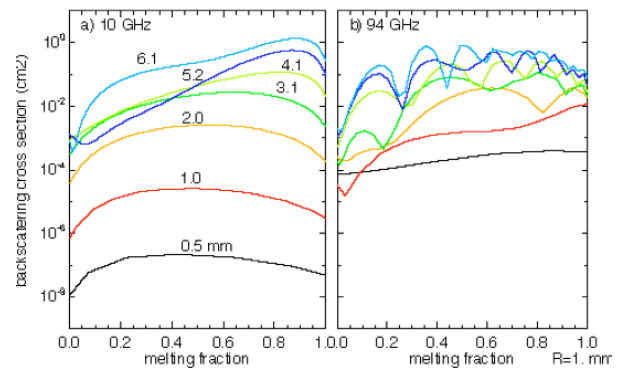


Fig. 4 Back-scattering cross-section at a) 10 GHz and b) 94 GHz as a function of melting ratio for selected melted drop diameters from 0.5 to 6.1 mm.

Figure 4 shows the profile of the calculated reflectivity and Doppler velocity for selected rainfall rate of 1 and 4 mm/hr. It reproduced the main features of the observed profiles around the melting layer. For rainfall rate less than 5 mm/hr, the reflectivity and Doppler velocity at 94 GHz are mostly contributed by the particles with melted diameter less than 2 mm. This explains the earlier stabilization of the 94 GHz Doppler velocity in the observation. The minimum reflectivity at 94GHz at the top of the melting layer is mostly due to the attenuation by snow particles, which could be as large as a few dB/km. In the lower part of the melting layer, the Doppler velocity at 94 GHz is larger than that at 10 GHz, which does not agree

with the observations. Further analysis will be shown at the conference.

Attenuation Retrieved from Dual-Wavelength Doppler Radar Observations. *J. Appl. Meteor.*, Submitted.

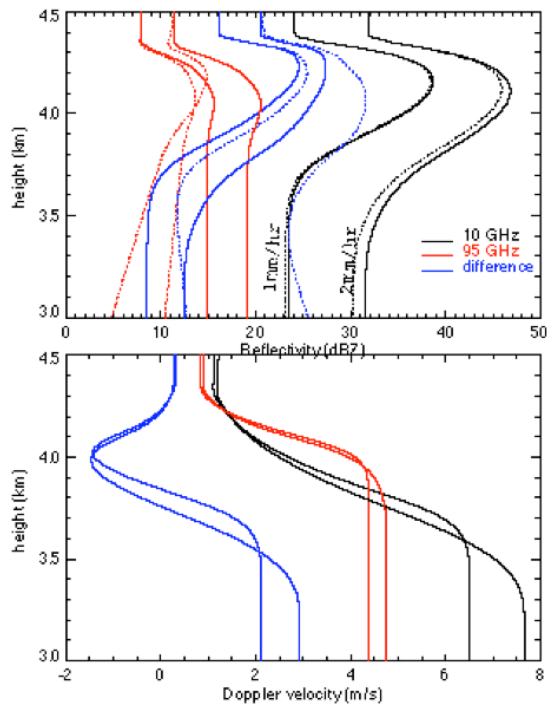


Fig. 5 a) Profile of calculated reflectivity at 10 GHz (red), 94 GHz (black) and the difference between the two frequencies (blue) for selected rainfall rate of 1 and 4 mm/hr. The dashed line is after taking into account the attenuation. b) Same as a) but for Doppler velocity.

### Acknowledgements

The authors thank Ed Zenker and Paul Racette for engineering support. This analysis has been supported by the NASA TRMM program.

### References

- Lhermitte, R., 1988: Observation of rain at vertical incidence with a 94 GHz Doppler radar: an insight on Mie scattering. *Geophys. Res. Lett.*, **15**, 1125-1128.
- Sassen K., J. R. Campbell, J. Zhu, P. Kollias, M. Shupe, and C. Williams, 2005: Lidar and triple-wavelength Doppler radar measurements of the melting layer: A revised model for dark- and brightband phenomena. *J. Appl. Meteor.*, **44**, 301-312.
- Tian, L., G. M. Hemsfield, Li, L., and R. C. Srivastava, 2005: Raindrop Size Distribution, Vertical Air Velocity and Water Vapor